Optimized Array-Based Spatially-Coupled LDPC Codes: An Absorbing Set Approach

Behzad Amiri*, Amirhossein Reisizadeh*, Jörg Kliewer†, and Lara Dolecek*
*Electrical Engineering Department, University of California, Los Angeles, Los Angeles, CA, USA
†Electrical and Computer Engineering Department, New Jersey Institute of Technology, Newark, NJ, USA
Emails: {amiri, reisizadeh}@ucla.edu, jkliewer@njit.edu, dolecek@ee.ucla.edu

***Abstract*—In the infinite blocklength regime, spatially-coupled LDPC codes are capable of achieving capacity-approaching performance under message-passing decoding. In the finite blocklength regime, it is known that absorbing sets compete with the codewords to be the output of sub-optimal message-passing decoders: the existence of such sets in the Tanner graph of LDPC codes causes performance degradation in the low error rate region. This paper presents a mathematical approach to finding the exact number of absorbing sets in array-based spatially-coupled (AB-SC) codes. Our analysis is universal in the sense that it is in principle applicable to absorbing sets of any size. Moreover, all design parameters of AB-SC codes such as the coupling length, the circulant size, and the cutting vector are considered in the presented count. Based on our analysis, we present an approach to find provably minimal cutting vectors, with respect to the number of absorbing sets, for the construction of AB-SC codes with various circulant sizes. Simulation results show the superior error floor performance of AB-SC codes with the minimal cutting vector compared to AB-SC codes with randomly-selected cutting vectors. We also provide the average number of non-binary absorbing sets in the Tanner graph of non-binary AB-SC codes constructed by uninformed (random) assignment of edge weights to a binary AB-SC code.**

I. Introduction

Spatially-coupled low-density parity-check (LDPC) codes are known to achieve the maximum-likelihood decoding threshold under belief-propagation decoding [1]. Thus, analysis and design of spatially-coupled LDPC codes have drawn a lot of recent attention, e.g., [2]–[6]. It has also been shown that non-binary spatially-coupled LDPC codes achieve the maximum-likelihood decoding threshold and have superior performance compared to their binary counterparts [7]–[9].

It is known that under message-passing algorithms, certain non-codewords result in failure in decoding of LDPC codes. *Absorbing sets (ASs)* are introduced in [10] as substructures of the Tanner graph which are responsible for the performance degradation of LDPC codes in the low error rate region. AS analyses and designs of array-based LDPC (AB-LDPC) codes with a reduced number of ASs are presented in [10], [11]. In the case of array-based spatially-coupled (AB-SC) codes, the authors in [12] show that the number of smallest ASs grows linearly with the coupling length L. Furthermore, the authors also show that the number of ASs in AB-SC codes is significantly less than the number of ASs in their underlying AB-LDPC codes. This observation suggests that AB-SC codes have better error floor performance compared to AB-LDPC codes.

In this work, we extend the results in [12] by: 1) introducing an analytical approach to find the exact number of ASs in AB-SC codes, 2) finding the minimal cutting vector, with respect to the number of absorbing sets, for AB-SC codes with arbitrary circulant size, and 3) finding the average number of non-binary ASs in non-binary AB-SC codes constructed by uninformed (random) assignment of edge weights to a binary AB-SC code. This set of tools are used to design spatially-coupled LDPC codes with superior performance in the error floor region.

II. Preliminaries and Definitions

In this section, we first review the construction of AB-SC codes using the edge spreading procedure [12]. We also briefly revisit the well-known definitions of binary and non-binary ASs [10], [13].

A. Array-based spatially-coupled LDPC codes

Assume that the following parameters are given:

- p: a prime number indicating the circulant size and the row weight,
- γ: the column weight,
- L: the coupling length,
- $\boldsymbol{\xi} = [\xi_0, \cdots, \xi_{\gamma-1}]$: the cutting vector[1] where $0 \leq \xi_0 < \xi_1 < \cdots < \xi_{\gamma-1} \leq p$.

We first construct the $\gamma p \times p^2$ underlying AB-LDPC code as follows:

$$H(\gamma, p) = \begin{bmatrix} I & I & I & ... & I \\ I & \sigma & \sigma^2 & \cdots & \sigma^{(p-1)} \\ \vdots & \vdots & \vdots & \ddots & \vdots \\ I & \sigma^{(\gamma-1)} & \sigma^{2(\gamma-1)} & \cdots & \sigma^{(p-1)(\gamma-1)} \end{bmatrix}, \quad (1)$$

where σ is a $p \times p$ circulant matrix formed by cyclically shifting all rows of the identity matrix one step to the left. The matrix $H(\gamma, p)$ can be viewed as a 2-D array of circulant submatrices where each row (column) of matrices denotes a row (column) group $i, 0 \leq i \leq \gamma - 1$ ($j, 0 \leq j \leq p - 1$). For our future discussions, we describe each column of $H(\gamma, p)$ by a pair (j, k) where j is the index of the column group, and k, $0 \leq k \leq p-1$ is the index of the column within the column group.

Based on the given cutting vector $\boldsymbol{\xi}$, the matrix H_0, with size $\gamma p \times p^2$, is formed by assigning each circulant matrix in $H(\gamma, p)$ with row group i and column group j, $j < \xi_i$, to

This work was supported by ASTC-IDEMA and NSF grants CCF-1161798 and CCF-1440001.

[1]Here we assume that $\xi_i, i \in \{0, 1, \cdots, \gamma - 1\}$ are distinct. In the general case, these parameters are not necessarily distinct.

the equivalent position in H_0. All other remaining elements of H_0 are then set to 0. Furthermore, matrix H_1 is defined as $H_1 = H(\gamma, p) - H_0$.

The parity-check matrix of an AB-SC code with the given coupling length L is then defined as

$$H(\gamma, p, L, \boldsymbol{\xi}) \triangleq \begin{bmatrix} H_0 & 0 & 0 & \cdots & 0 & 0 \\ H_1 & H_0 & 0 & \cdots & 0 & 0 \\ 0 & H_1 & H_0 & \cdots & 0 & 0 \\ \vdots & \vdots & \ddots & \ddots & \vdots & \vdots \\ 0 & 0 & 0 & \cdots & H_1 & H_0 \\ 0 & 0 & 0 & \cdots & 0 & H_1 \end{bmatrix}. \quad (2)$$

Note that in the above construction, the syndrome former memory m_s is assumed to be 1. In the general case, where $m_s \geq 1$, we have $H(\gamma, p) = H_0 + H_1 + \cdots + H_{m_s}$. Figure 1 shows an example of the AB-SC code construction where $\gamma = 3$, $p = 11$, $L = 2$, and $\boldsymbol{\xi} = [3, 6, 9]$. For the sake of our later discussion, we define a region $R_n, n \in \{1, \cdots, \gamma + 1\}$ in $H(\gamma, p)$ as the set of column groups with indices between ξ_{n-2} and ξ_{n-1}. We assume $\xi_{-1} = 0$ and $\xi_\gamma = p$. The number of column groups within the region $R_n, n \in \{1, \cdots, \gamma+1\}$ is denoted by r_n. The definition of regions can be expanded to AB-SC codes, where each region is similarly defined as the set of column groups between two consecutive edges of the cutting vector. Figure 1 illustrates an example of regions for column weight 3 AB-LDPC and AB-SC codes.

The following definition describes the construction of non-binary AB-SC codes.

Definition 1. *For a given parity-check matrix $H(\gamma, p)$ of a binary AB-LDPC code, the parity-check matrix $H_q(\gamma, p)$ of a non-binary AB-LDPC code over GF(q) is constructed by replacing the elements with value '1' of $H(\gamma, p)$ with non-zero elements of GF(q). The parity-check matrix $H_q(\gamma, p, L, \boldsymbol{\xi})$ of a non-binary AB-SC code is then constructed by the same edge spreading procedure as above.*

B. Binary and non-binary absorbing sets

Consider a subgraph of a Tanner graph over GF(q) induced by a variable nodes (VNs), given by the node set $\mathcal{V}$.

Definition 2. ([13]) *The set $\mathcal{V}$ is an (a, b) AS over GF(q) if there exists an input $(v_1, v_2, \cdots, v_a) \in$ GF(q)^a for the VNs in $\mathcal{V}$ such that there exist exactly b unsatisfied check nodes (CNs) connected to the VNs in $\mathcal{V}$, and with the property that, for each VN, the number of connected satisfied checks is greater than the number of connected unsatisfied checks.*

Note that if $q = 2$ (binary code), the above definition can be simplified as follows.

Definition 3. [10] *The set $\mathcal{V}$ is an (a, b) binary AS if there are b odd degree CNs connected to the VNs in $\mathcal{V}$ and each VN is connected to more even degree CNs than odd degree ones.*

Elementary ASs are a subset of ASs where each of their satisfied (unsatisfied) CNs has exactly two edges (one edge) connected to the VNs in $\mathcal{V}$. In the elementary case, the conditions of ASs over GF(q) can be simplified as follows.

Lemma 1. ([13]) *A subset of VNs $\mathcal{V}$ is an elementary AS over GF(q) if and only if:*

1) *(Topological condition) For the induced subgraph corresponding to $\mathcal{V}$ and its neighboring CNs, unlabeling of all edges (converting all edge weights to one) results in a binary elementary AS.*
2) *(Weight condition) For every cycle of length $2s$, the weights of the edges w_i, $i \in \{1, 2, \ldots, 2s\}$, satisfy:*

$$\prod_{k=1}^{s} \mathrm{w}_{2k-1} = \prod_{k=1}^{s} \mathrm{w}_{2k} \mod q. \quad (3)$$

III. Exact Enumeration of Binary Absorbing Sets in Array-Based Spatially-Coupled Codes

In this section, we introduce an approach to calculate the exact number of binary absorbing sets existing in the Tanner graph of binary AB-SC codes. Although our procedure is applicable to any column weight, for the ease of discussion, we limit our analysis to column weight 3 codes. Extension of these results to column weight 4 AB-SC codes and larger AS sizes can be found in [15].

We first revisit the bit, check and pattern consistency conditions in AB-LDPC codes.

Lemma 2. ([10]) ***Bit consistency:*** *The neighboring CNs of a VN must have distinct row-group (i) indices.*
Check consistency: *The neighboring VNs of a CN must have distinct column-group (j) indices.*
Pattern consistency: *If two VNs corresponding to columns (j_1, k_1) and (j_2, k_2) share a CN c_1 in row group i_1, then:*

$$k_1 + i_1 j_1 = k_2 + i_1 j_2 \mod p. \quad (4)$$

Remark 1. *By virtue of spatially coupling, each CN can only be connected to VNs that belong to γ consecutive regions. In addition to the pattern consistency condition, this property of AB-SC codes imposes extra constraints on the valid choices for column group indices of two connected VNs.*

The following example clarifies Remark 1.

Example 1. *Consider the $H(3, 11, 2, [3, 6, 9])$ parity-check matrix in Figure 1(b). If two VNs share a CN in the second row group ($i = 1$), then the regions which the two VNs belong to should be within the set $\{R'_1, R'_2\}$. Assuming that v_1 belongs to R'_1 with width $r_1 = 3$ and v_2 belongs to R'_2 with width $r_2 = 3$, the following three conditions should be satisfied:*

$$k_1 + j_1 = k_2 + j_2 \mod p, \quad 0 \leq j_1 \leq 2, \quad 3 \leq j_2 \leq 5.$$

The following lemma presents the size of the minimal ASs in AB-SC codes with column weight 3.

Lemma 3. ([12]) *The minimal possible AS in the Tanner graph of $H(3, p, L, \xi)$ has size $(3, 3)$.*

Since the minimal ASs typically contribute the most to the error floors of LDPC codes, we focus our analysis on $(3, 3)$ ASs. In [12], the authors show that the number of (minimal) $(3, 3)$ absorbing sets in column weight-3 AB-SC codes grows linearly with the coupling length L. Through our analysis, we provide the exact count of $(3, 3)$ ASs in the Tanner graph corresponding to $H(3, p, L, \boldsymbol{\xi})$, as a function of circulant size p, coupling length L, and the cutting vector $\boldsymbol{\xi}$.

We consider the $(3, 3)$ AS structure shown in Figure 2. Without loss of generality, we assume that v_1 and v_2 share

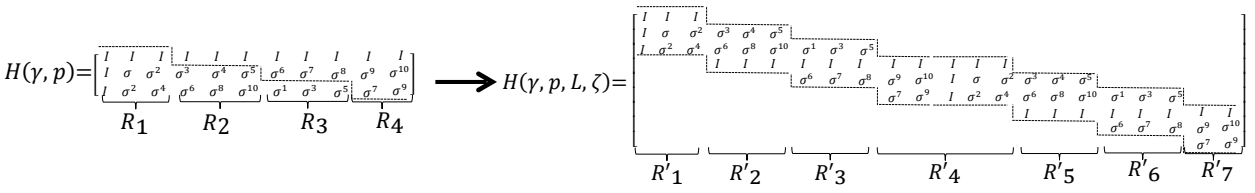

(a) (b)

Fig. 1. (a) Example of AB-LDPC codes with $p = 11$ and $\gamma = 3$, (b) Example of AB-SC codes with $p = 11$, $\gamma = 3$, $L = 2$, and cutting vector $\boldsymbol{\xi} = [3, 6, 9]$. Here, $r_i = |R_i|$ for $i \in \{1, 2, 3, 4\}$ and $r'_i = |R'_i|$ for $i \in \{1, 2, \cdots, 7\}$. Moreover, $r'_1 = r_1$, $r'_2 = r_2$, $r'_3 = r_3$, $r'_4 = r_4 + r_1$, $r'_5 = r_2$, $r'_6 = r_3$, and $r'_7 = r_4$.

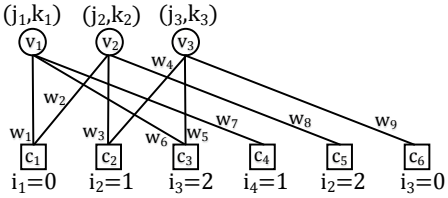

Fig. 2. Structure of a $(3, 3)$ AS over GF(q). Note that in the binary case, w_1 through w_9 are equal to '1'.

a CN in the row group $i_1 = 0$, v_2 and v_3 share a CN in the row group $i_2 = 1$, and v_1 and v_3 share a CN in the row group $i_3 = 2$. Thus the pattern consistency constraints lead to:

$$k_1 + 2j_1 = k_3 + 2j_3, \quad k_1 = k_2, \quad k_2 + j_2 = k_3 + j_3,$$

where j_1, j_2, j_3, k_1, k_2, and k_3 are in $\{0, 1, \cdots, p-1\}$ and all equations are modulo p. The above equations result in the following equation, purely on indices of column groups:

$$j_2 = 2j_1 - j_3 \mod p. \tag{5}$$

It is shown in [10] that by fixing the values of j_1, j_3, and k_1 in the above equations, the values of all other variables can be uniquely determined. In the case of AB-LDPC codes, j_1 and j_3 can take any pair of unequal values between 0 and $p-1$. Therefore, there exist $p^2(p-1)$ minimal $(3, 3)$ ASs (p choices for k_1) in column weight 3 AB-LDPC codes. Through our analysis below, we show that not all pairs of (j_1, j_3) are valid in the case of AB-SC codes; this results into a fewer number of $(3, 3)$ absorbing sets under spatial coupling.

Lemma 4. *The three VNs in a $(3, 3)$ AS span at most three consecutive regions.*

Proof. Based on Remark 1 and the fact that each pair of VNs in a $(3, 3)$ AS are connected through a satisfied CN (Figure 2), the three VNs span at most three consecutive regions. □

Lemma 4 enables us to categorize all $(3, 3)$ ASs in $H(3, p, L, \boldsymbol{\xi})$ into four exhaustive, mutually-exclusive cases[2]:

Case 1: All three VNs are in the same region.

Case 2: Two VNs are in the same region, the third VN is in the next region.

Case 3: Two VNs are in the same region, the third VN is in the previous region.

Case 4: Each of the three VNs belong to a different region and the three regions are consecutive.

(a) Number of ASs in Case 1: In this case, we put a 'search window' over each region (R'_1 to R'_{3L+1}) and count the number of $(3, 3)$ ASs within that region.

[2]It is trivial to show that due to the check consistency property of AB-LDPC codes [10], it is not possible to have two VNs in the same region R_n and the third VN in the region R_{n-2} or R_{n+2}.

Lemma 5. *The total number of $(3, 3)$ ASs in Case 1, denoted by $F_1(p, L, r_1, r_2, r_3, r_4)$, is obtained as follows:*

$$F_1(p, L, r_1, r_2, r_3, r_4) = F_1^{R_1}(p, r_1) + L \cdot F_1^{R_1}(p, r_2) + (L-1) \cdot F_1^{R_1}(p, r_1 + r_4) + L \cdot F_1^{R_1}(p, r_3) + F_1^{R_1}(p, r_4), \tag{6}$$

where $F_1^{R_n}(p, m)$ is the count of $(3, 3)$ ASs within region R_n of width m, for a given circulant size p.

Proof. The total number of $(3, 3)$ ASs in Case 1 is equal to the summation of the number of absorbing sets within regions R'_1 through R'_{3L+1}, i.e.,

$$F_1(p, L, r_1, r_2, r_3, r_4) = \sum_{n=1}^{3L+1} F_1^{R'_n}(p, r'_n). \tag{7}$$

One can show that

$$F_1^{R_1}(p, m) = F_1^{R'_n}(p, m), n \in \{1, \cdots, 3L+1\}. \tag{8}$$

By substituting each term in (7) with LHS of (8), and by the facts that

$$r'_1 = r_1, \{k : (k \mod 3) = 2\} \to r'_k = r_2,$$
$$r'_{3L+1} = r_4, \{k : (k \mod 3) = 0\} \to r'_k = r_3,$$
$$\{k : (k \mod 3) = 1, k \neq 1, k \neq 3L+1\} \to r'_k = r_1 + r_4,$$

Equation (6) is obtained. □

As an example, we consider that all the VNs are in region R'_1. The problem of counting the valid values for j_1 and j_3 can be graphically interpreted as the problem of counting the integer pairs (j_1, j_3) within the areas S_1, S_2, and S_3 in Figure 3(a). Note that based on the values of p and r_1, each of the areas S_2 and S_3 can be either the empty set $\varnothing$ or a triangle. The number of (integer) points existing in S_1, S_2, and S_3, denoted by $N_{S_1}(r_1)$, $N_{S_2}(p, r_1)$, and $N_{S_3}(p, r_1)$, respectively, can be found by (for brevity, details are omitted)

$$N_{S_1}(r_1) = \begin{cases} \frac{(r_1-1)^2}{2} \text{ if } r_1 \text{ is odd,} \\ \frac{r_1(r_1-2)}{2} \text{ if } r_1 \text{ is even,} \end{cases}$$

and

$$N_{S_2}(p, r_1) = N_{S_3}(p, r_1) = \begin{cases} \frac{(2r_1-p)^2-1}{4} \text{ if } 2r_1 \geq p+2, \\ 0 \text{ if } 2r_1 < p+2. \end{cases}$$

Therefore, the total number of ASs within region R_1 is

$$F_1^{R_1}(p, r_1) = p \cdot (N_{S_1}(r_1) + N_{S_2}(p, r_1) + N_{S_3}(p, r_1)). \tag{9}$$

Note that the multiplication by p in (9) is due to the p choices for k_1. As an example, if $p = 11$ and $r_1 = 8$, the number of $(3, 3)$ ASs with all their three variable nodes in region 1 is equal to $11 \times (24 + 6 + 6) = 386$.

(b) Number of ASs in Case 2: Here, we put a 'search window' over each two consecutive regions ($\{R'_1, R'_2\}$ through $\{R'_6, R'_7\}$).

Lemma 6. *The total number of $(3, 3)$ ASs in Case 2 is:*

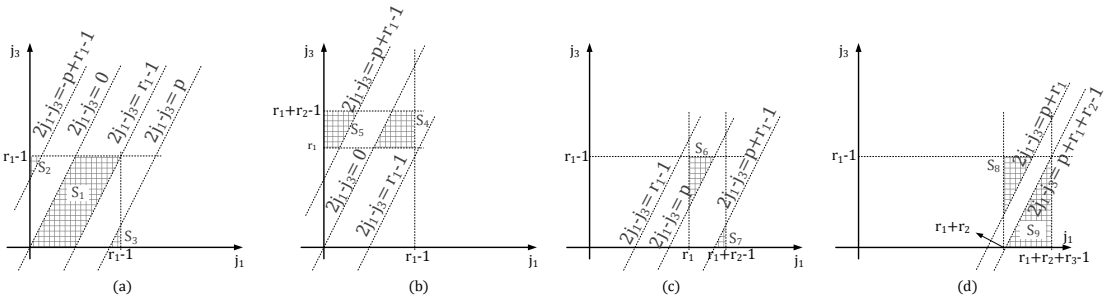

Fig. 3. (a) Example of Case 1. All VNs in region R'_1. (b) Example of Case 2. VNs 1 and 2 are in region R'_1 and VN 3 is in region R'_2. (c) Example of Case 3. VN 3 is in region R'_1 and VNs 1 and 2 are in region R'_2. (d) Example of Case 4. VN 3 is in region R'_1, VN 2 is in region R'_2 and VN 1 is in region R'_3.

$$F_2(p,L,r_1,r_2,r_3,r_4) = F_2^{R_1}(p,r_1,r_2) + L\cdot F_2^{R_2}(p,r_2,r_3) + (L-1)\cdot F_2^{R_3}(p,r_3,r_1+r_4) + (L-1)\cdot F_2^{R_1}(p,r_1+r_4,r_2) + F_2^{R_3}(p,r_3,r_4), \quad (10)$$

where $F_2^{R_n}(p,m,k)$ denotes the number of $(3,3)$ ASs with two VNs in R_n of width m and one VN in R_{n+1} of width k.

A complete discussion of the calculation for each term in the RHS of (10) as well as for the related terms $F_3^{R_{1/2/3}}$ and $F_4^{R_{1/2/3}}$ below in Lemma 7 and 8, respectively, can be found in [14].

As an example, the valid areas for the (j_1, j_3) pair when VNs 1 and 2 are in R_1, and VN 3 is in R_2 are shown in Figure 3(b). Note that based on the values of p, r_1, and r_2, areas S_4 and S_5 can be empty set $\varnothing$, a triangle, or a trapezoid.

(c) Number of ASs in Case 3: Similar to Case 2, we put a 'search window' over each two consecutive regions. Here, we count the number of $(3,3)$ ASs which have two VNs in the second region and one VN in the first region.

Lemma 7. *The total number of $(3,3)$ ASs in Case 3:*

$$F_3(p,L,r_1,r_2,r_3,r_4) = F_3^{R_1}(p,r_1,r_2) + L\cdot F_3^{R_2}(p,r_2,r_3) + (L-1)\cdot F_3^{R_3}(p,r_3,r_1+r_4) + (L-1)\cdot F_3^{R_1}(p,r_1+r_4,r_2) + F_3^{R_3}(p,r_3,r_4), \quad (11)$$

where $F_3^{R_n}(p,m,k)$ is the count of $(3,3)$ ASs with one VN in R_n of width m and two VNs in R_{n+1} of width k.

As an example of Case 3, we plotted the areas for the (j_1, j_3) pair when VN 2 and VN 3 are in R_1 and VN 1 is in R_2 in Figure 3(c). Again based on the values of p, r_1, and r_2, areas S_6 and S_7 can be $\varnothing$, a triangle or a trapezoid.

(d) Number of ASs in Case 4: Here, we put a 'search window' over each three consecutive regions. For each window, we count the number of $(3,3)$ ASs which have one VN in each region.

Lemma 8. *The total number of $(3,3)$ ASs in Case 4:*

$$F_4(p,L,r_1,r_2,r_3,r_4) = (L-1)\cdot F_4^{R_2}(p,r_2,r_3,r_1+r_4) + F_4^{R_1}(p,r_1,r_2,r_3) + (L-1)\cdot F_4^{R_3}(p,r_3,r_1+r_4,r_2) + (L-1)\cdot F_4^{R_1}(p,r_1+r_4,r_2,r_3) + F_4^{R_2}(p,r_2,r_3,r_4), \quad (12)$$

where $F_4^{R_n}(p,m,k,\ell)$ is the count of $(3,3)$ ASs with one VN in R_n of width m, one VN in R_{n+1} of width k and one VN in R_{n+2} of width ℓ.

As an example, in Figure 3(d), we plotted the valid areas for the (j_1, j_3) pair when VN 3 is in R_1 and VN 2 is in R_2 and VN 1 is in R_3. Again based on the values of p, r_1, r_2, and r_3, areas S_8 and S_9 can be $\varnothing$, a triangle, or a trapezoid.

For a given circulant size p, a coupling length L, and a cutting vector $\boldsymbol{\xi}$, the following equation provides the total number of $(3,3)$ ASs, which is denoted by $A_{(3,3)}(3,p,L,\boldsymbol{\xi})$:

$$A_{(3,3)}(3,p,L,\boldsymbol{\xi}) = \sum_{n=1}^{4} F_n(p,L,r_1,r_2,r_3,r_4), \quad (13)$$

where $r_1 = \xi_1$, $r_2 = \xi_2 - \xi_1$, $r_3 = \xi_3 - \xi_2$ and $r_4 = p - \xi_3$, and functions $F_n(p,L,r_1,r_2,r_3,r_4), n = \{1,2,3,4\}$ are calculated as in (6), (10), (11), and (12).

Remark 2. *The AS enumeration method presented in this section can be applied to any (a,b) AS. However, for larger ASs, the problem is more involved as the problem of finding the valid points for column group indices must be formulated over higher dimensional spaces. This is due to the fact that for larger ASs, column group indices can not necessarily be specified as a function of only two column groups indices [15].*

IV. Minimal Cutting Vector for AB-SC Codes

In this section, we provide the minimal cutting vector, with respect to the number of ASs, for AB-SC codes.

Definition 4. ([12]) *For any given circulant size p, a minimal cutting vector corresponding to size (a,b) AS is defined as $\boldsymbol{\xi}^*_{(a,b)}(p) = \arg\min_{\boldsymbol{\xi}} \lim_{L\to\infty} A_{(a,b)}(\gamma,p,L,\boldsymbol{\xi})$.*

Theorem 1. *A minimal cutting vector for $(3,3)$ ASs in column weight 3 AB-SC codes with circulant size p is*

$$\boldsymbol{\xi}^*_{(a,b)}(p) = \arg\min_{\boldsymbol{\xi}}\{F_1^{R_1}(p,r_2) + F_1^{R_1}(p,r_1+r_4) + F_1^{R_1}(p,r_3) + F_2^{R_2}(p,r_2,r_3) + F_2^{R_3}(p,r_3,r_1+r_4) + F_2^{R_1}(p,r_1+r_4,r_2) + F_3^{R_2}(p,r_2,r_3) + F_3^{R_3}(p,r_3,r_1+r_4) + F_3^{R_1}(p,r_1+r_4,r_2) + F_4^{R_2}(p,r_2,r_3,r_1+r_4) + F_4^{R_3}(p,r_3,r_1+r_4,r_2) + F_4^{R_1}(p,r_1+r_4,r_2,r_3)\}, \quad (14)$$

where $r_1 = \xi_1$, $r_2 = \xi_2 - \xi_1$, $r_3 = \xi_3 - \xi_2$ and $r_4 = p - \xi_3$ and the functions are shown in Lemma 5, 6, 7, and 8.

Proof. As $L \to \infty$, the terms in (6), (10), (11), and (12) which grow linearly with L become dominant terms. By summing these dominant terms, we obtain the RHS of (14). □

Remark 3. *Based on Theorem 1, the problem of finding the minimal cutting vector is essentially mapped to finding an integer vector which minimizes the function in* (14)*. Compared to [12], where the minimal cutting vector for $p \leq 23$ is found by exhaustive computer search, our approach is computationally*

TABLE I
MINIMAL CUTTING VECTORS FOR VARIOUS CIRCULANT SIZES.

p	Minimal cutting vector
67	[15, 31, 47]
97	[23, 48, 73]
107	[28, 54, 81]
113	[29, 57, 88]

TABLE II
$(3,3)$ AS COMPARISON FOR VARIOUS CUTTING VECTORS, $p = 67$, $L = 2$.

Optimal	Random ([10, 18, 56])	Average
273561	379957	441293

less complex and provides the minimal cutting vector for large choices of p. As an example, a list of minimal cutting vectors for $p = 67, 97, 107, 113$ is provided in Table I.

Table II compares the number of $(3,3)$ ASs for the minimal cutting vector with a randomly selected cutting vector when $L = 2$ and $p = 67$. Table II also includes the average number of ASs over all possible selections of cutting vectors for $H(3, p, L, \boldsymbol{\xi})$. It can be observed that the minimal cutting vector reduces the number of $(3,3)$ ASs by $\approx 39\%$ compared to the average number of ASs over all possible cutting vectors. Figure 4 shows the performance comparison between the codes constructed using the cutting vectors in Table II, when the coupling length[3] $L = 100$ and a sliding window decoder implemented based on the soft-xor algorithm is employed. The code with the minimal cutting vector shows about one order of magnitude performance improvement in the error floor region, compared to the code with randomly selected cutting vector.

V. AS ANALYSIS FOR NON-BINARY AB-SC CODES

In this section, we provide the average number of $(3,3)$ non-binary ASs in non-binary AB-SC codes.

Theorem 2. *Consider an AB-SC code over GF(q), with the circulant size p, the coupling length L, the cutting vector $\boldsymbol{\xi}$, and the random assignment of edge weights. The number of $(3,3)$ non-binary ASs, averaged over all possible edge weight assignments, denoted by $\overline{A}^{q}_{(3,3)}(3, p, L, \boldsymbol{\xi})$, is*

$$\overline{A}^{q}_{(3,3)}(3, p, L, \boldsymbol{\xi}) = \frac{1}{(q-1)} \sum_{n=1}^{4} F_n(p, L, r_1, r_2, r_3, r_4), \quad (15)$$

where $r_1 = \xi_1$, $r_2 = \xi_2 - \xi_1$, $r_3 = \xi_3 - \xi_2$ and $r_4 = p - \xi_3$, and the functions $F_n(p, L, r_1, r_2, r_3, r_4), n = \{1, 2, 3, 4\}$ are calculated in (6)*,* (10)*,* (11) *and* (12)*.*

Proof. Consider the structure in Figure 2 with non-binary edge weights w_1 through w_6. There exist $(q-1)^6$ unique choices for the set of six edge weights. Based on the weight condition of non-binary ASs in (3), the edge weight in a non-binary AS satisfy $\mathrm{w}_1\mathrm{w}_3\mathrm{w}_5 = \mathrm{w}_2\mathrm{w}_4\mathrm{w}_6 \mod q$. By choosing w_1 through w_5 independently from $GF(q)/0$, edge weight w_6 can be uniquely determined. Thus, there exist $(q-1)^5$ choices for edge weights which result in an AS over GF(q). As a result, the average number of $(3,3)$ non-binary ASs is equal to

$$\frac{(q-1)^5}{(q-1)^6} A_{(3,3)}(3, p, L, \boldsymbol{\xi}) = \frac{1}{(q-1)} \sum_{n=1}^{4} F_n(p, L, r_1, r_2, r_3, r_4).$$

□

Note that the non-binary edge weights provide new degrees of freedom to the design of AB-SC codes. In particular, by manipulating the edge weights so that the weight condition is violated for at least one cycle in each non-binary AS, we provably eliminate non-binary AS in non-binary AB-SC codes. The AS reduction in SC codes by informed selection of non-binary edge weights is a subject of our ongoing research.

[3]The code length is 448900 bits and the rate is 0.94. The rate of the original AB-LDPC code is 0.95.

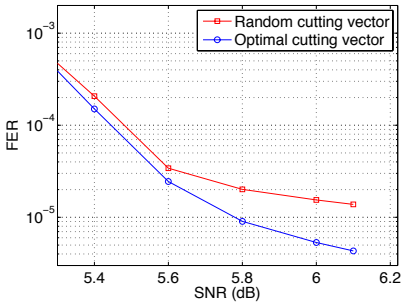

Fig. 4. Performance comparison for the codes constructed by the cutting vectors presented in Table II, with constraint length 4489 bits, column weight 3 and $L = 100$.

VI. CONCLUSION

In this paper, we first introduced an analytical method to enumerate ASs in the Tanner graph of AB-SC codes. Based on our AS enumeration, we found the minimal cutting vector, which minimizes the number of ASs for any choice of the circulant size in AB-SC codes. In our example, we showed that compared to the average number of ASs over all possible cutting vectors, choosing the minimum cutting vector results in approximately 39% reduction in the number of ASs. We also provided the average number of $(3,3)$ ASs in AB-SC codes over GF(q).

REFERENCES

[1] S. Kudekar, T. Richardson, and R. Urbanke, "Spatially coupled ensembles universally achieve capacity under belief propagation," *IEEE Trans. Inf. Theory*, vol. 59, no. 12, pp. 7761-7813, Dec. 2013.

[2] M. Lentmaier *et al.*, "Iterative decoding threshold analysis for LDPC convolutional codes," *IEEE Trans. Inf. Theory*, vol. 56, no. 10, pp. 5274-5289, Oct. 2010.

[3] D. G. M. Mitchell, A. E. Pusane, and D. J. Costello, Jr., "Minimum distance and trapping set analysis of protograph-based LDPC convolutional codes," *IEEE Trans. Inf. Theory*, vol. 59, pp. 254-281, Jan. 2013.

[4] M. Stinner, P. M. Olmos, "Analyzing finite-length protograph-based spatially-coupled LDPC codes," in *Proc. IEEE ISIT*, 2014.

[5] K. Kasai and K. Sakaniwa, "Spatially-coupled MacKay-Neal codes and Hsu-Anastasopoulos codes," *IEICE Trans. Fundamentals*, vol. E94-A, no. 11, pp. 2161-2168, Nov. 2011.

[6] N. Obata, Y.-Y. Jian, K. Kasai, and H. D. Pfister, "Spatially-coupled multiedge type LDPC codes with bounded degrees that achieve capacity on the BEC under BP decoding," in *Proc. IEEE ISIT*, 2013.

[7] I. Andriyanova and A. Graell i Amat, "Threshold saturation for non-binary SC-LDPC codes on the binary erasure channel," *Submitted to IEEE Trans. on Inf. Theory*, 2013.

[8] L. Wei *et al.*, "Design of spatially-coupled LDPC codes over GF(q) for windowed decoding," *Submitted to IEEE Trans. on Inf. Theory*, 2014.

[9] K. Huang *et al.*, "Performance comparison of LDPC block and spatially-coupled codes over GF(q)," *Submitted to IEEE TCOM*, 2014.

[10] L. Dolecek *et al.*, "Analysis of absorbing sets and fully absorbing sets of array-based LDPC codes," *IEEE Trans. on Inf. Theory*, vol. 56, no. 1, pp. 181-201, Jan. 2010.

[11] J. Wang, L. Dolecek and R. Wesel, "The cycle consistency matrix approach to absorbing sets in separable circulant-based LDPC codes," *IEEE Trans. on Inf. Theory*, vol. 59, no. 4, pp. 2293-2314, Apr. 2013.

[12] D. G. M. Mitchell, L. Dolecek, and D. J. Costello, Jr., "Absorbing set characterization of array-based spatially-coupled LDPC codes," in *Proc. IEEE ISIT*, 2014.

[13] B. Amiri, J. Kliewer, and L. Dolecek, "Analysis and enumeration of absorbing sets for non-binary graph-based codes," *IEEE TCOM*, vol. 62, no. 2, pp. 398-409, Feb. 2014.

[14] B. Amiri *et al.*, "Optimized array-based spatially-coupled LDPC codes: an absorbing set approach," [Online]. Available: http://amiri.bol.ucla.edu/TechnicalReport.pdf

[15] B. Amiri *et al.*, "Optimized design of finite-length spatially-coupled codes: an absorbing set-based analysis," *Submitted to IEEE Journal on Selected Areas in Commun. (JSAC)*, 2015.